

Serotonin 2A Receptor Attenuates Psoriatic Inflammation by Suppressing IL-23 Secretion in Monocyte-derived Langerhans Cells

Supplemental Information

Figure S1.

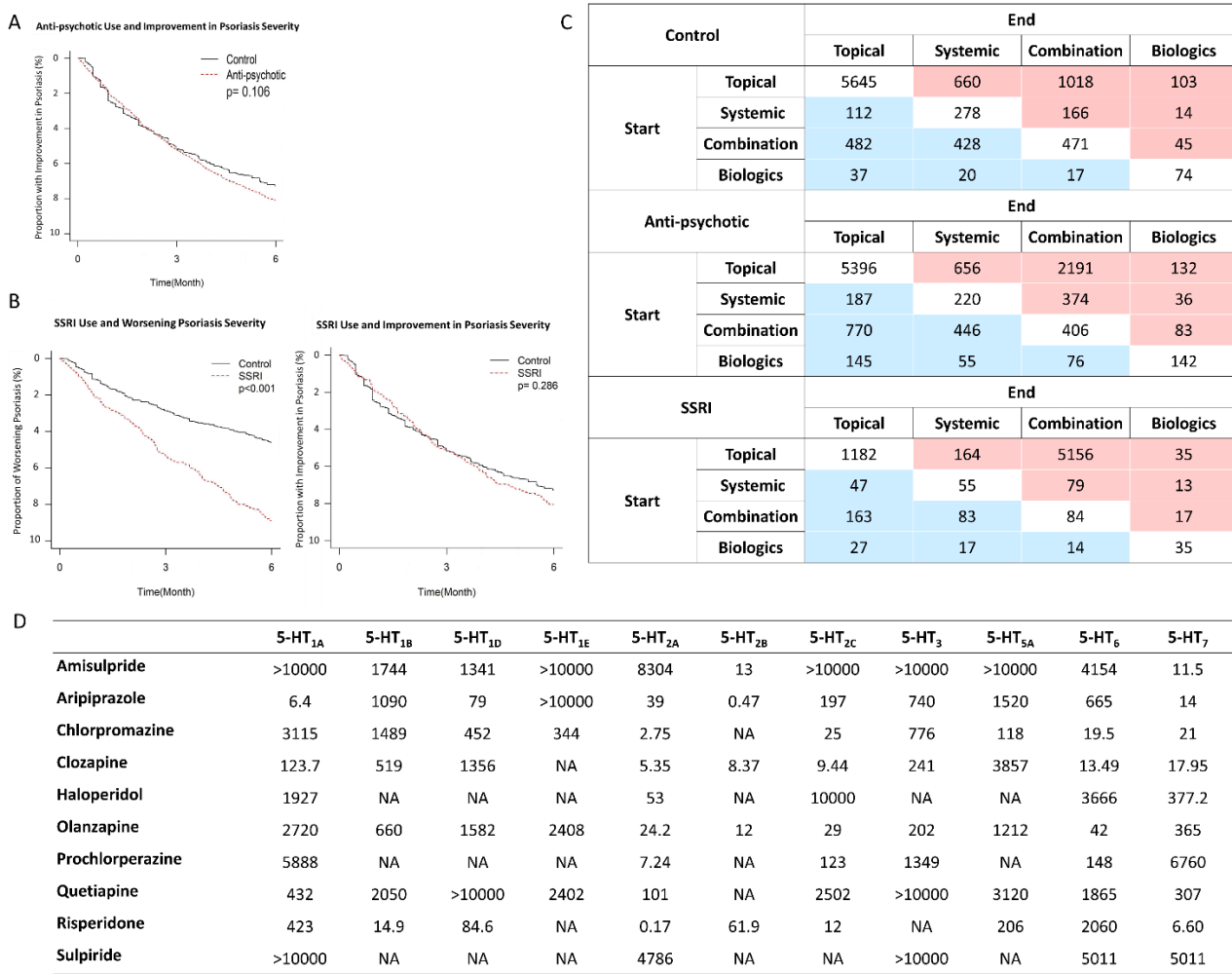


Figure S1. Anti-psychotic and SSRI use worsen psoriatic outcomes. Related to Figure 1. A) Kaplan-Meier plot of anti-psychotic use with improvement in psoriasis outcome. B) Kaplan-Meier plots of Selective Serotonin Reuptake Inhibitor (SSRI) use with worsening or improving psoriasis outcome. C) Table showing the number of patients in each category of psoriatic treatment received (as a surrogate for severity with topical the least severe and biologics the most severe) before anti-psychotic or SSRI use (Start, row) and psoriatic treatment received 6 months after anti-psychotic or SSRI use (End, column) with aged-matched and gender-matched controls. Red represents a worsened outcome, white represents no change, and blue represents an improvement in outcome. D) Table showing inhibitory constant (K_i in nM) of each anti-psychotic to each serotonin receptor. Data collected from PDSP K_i Database.

Figure S2.

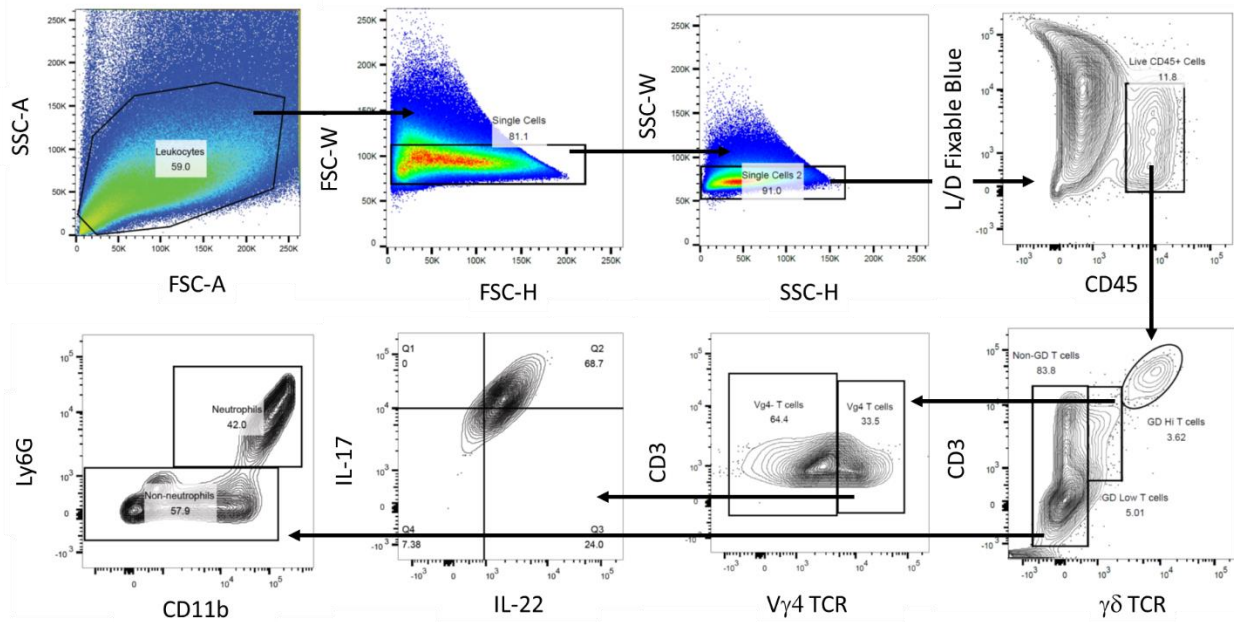


Figure S2. Gating strategy for flow cytometry of $\gamma\delta$ T cells and neutrophils. Related to Figure 2.
Figure showing the gating strategy of identifying various Langerhans cell subsets.

Figure S3.

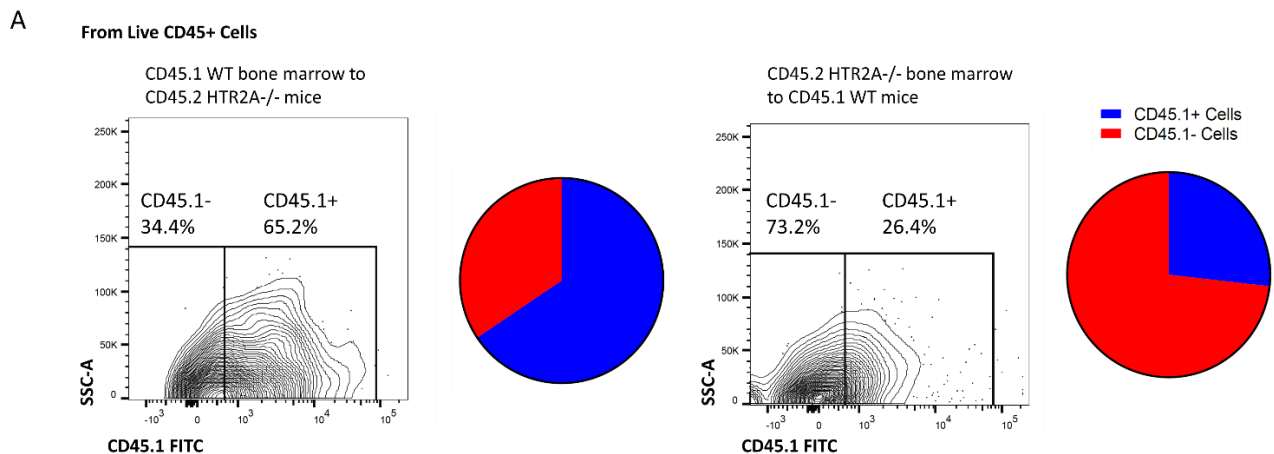


Figure S3. The composition of cells changed after bone marrow transplant. Related to Figure 2.

A) Representative figure with pie charts showing the composition of CD45.1+ cells and CD45.1- cells in CD45.2 HTR2A-/ mice transplanted with CD45.1 wild type bone marrow and vice versa.

Figure S4.

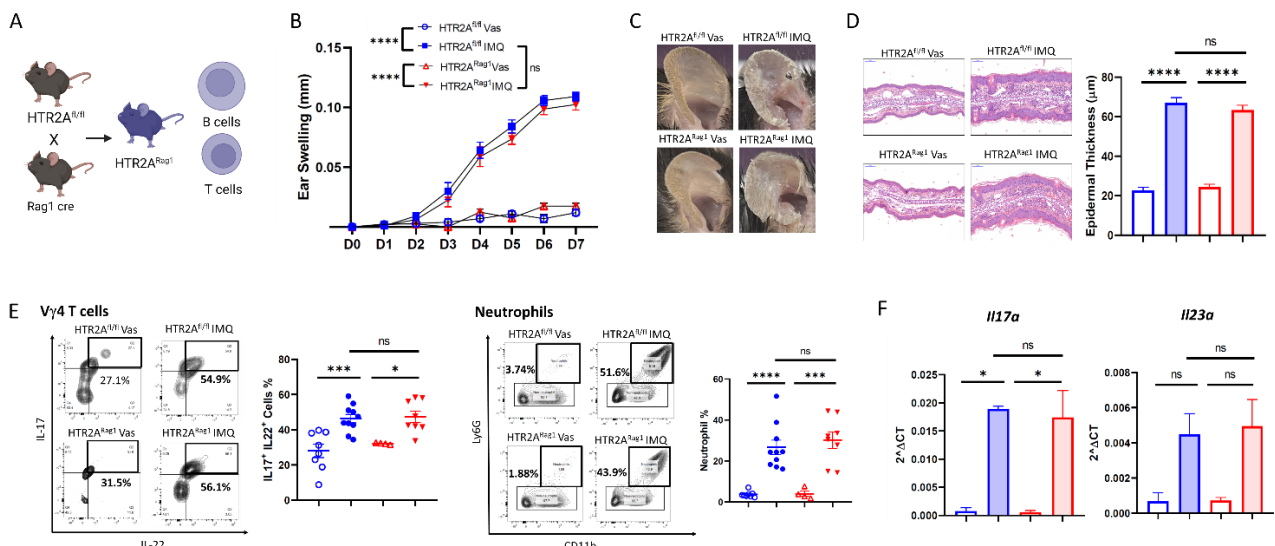


Figure S4. HTR2A deficiency in adaptive immune cells does not exacerbate inflammation. A) Schematic showing strategy for developing conditional knockout mice with deficient HTR2A in adaptive immune cells only by crossing HTR2A floxed mice with Rag1 cre mice. B) Line chart showing changes in ear swelling of mice. (n=4 to 8) C) Pictures showing ears of mice of various groups on Day 7. D) H&E-stained slides with quantification of epidermal thickness. E) Flow cytometry of IL17⁺ IL22⁺ V γ 4 T cells and neutrophils in the respective groups with quantifications. F) qPCR of pro-inflammatory cytokines of respective groups. Data are representative of two independent experiments (B-F). p values determined by two-way ANOVA (B) followed by Tukey's post-hoc test and one-way ANOVA (D-F) followed by Tukey's post-hoc test. Mean \pm SEM (D-F). *, p<0.05; ***, p<0.001; ****, p<0.0001; ns, non-significant.

Figure S5.

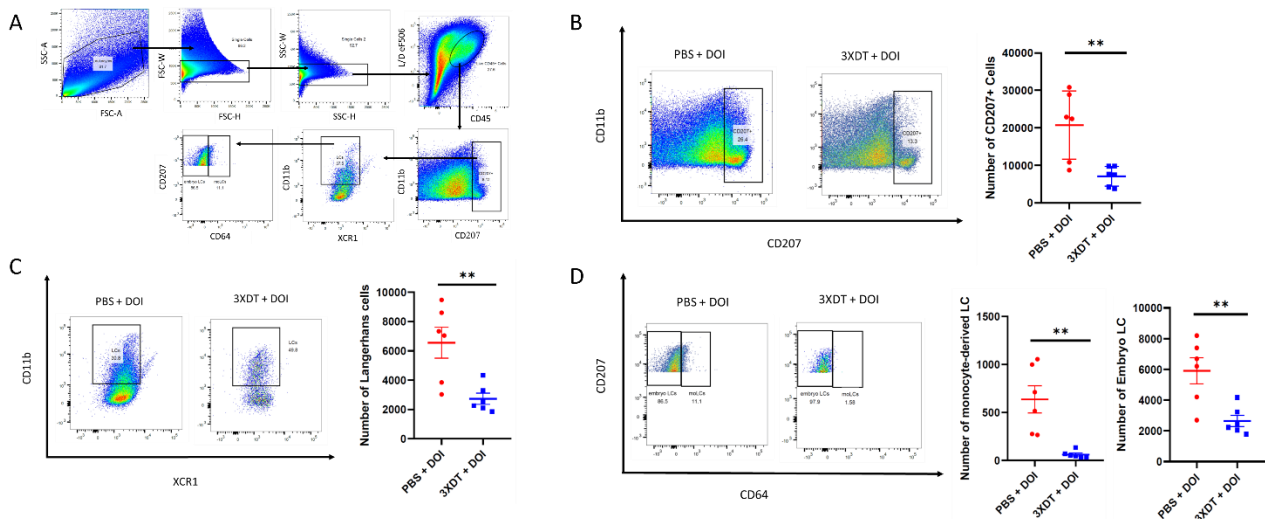


Figure S5. Depletion of different Langerhans cell subsets using varying doses of diphtheria toxin.

Related to Figure 4. A) Figures showing the gating strategy of identifying various Langerhans cell subsets. B) Dot plot showing the number of CD207+ cells with quantification. (n=4) C) Dot plot showing the number of Langerhans cells with quantification. D) Dot plot showing the number of monocyte-derived Langerhans cells and embryo Langerhans cells with quantification. Data are representative of two independent experiments (B-D). p values determined by unpaired Student's T-Test (B-D). Mean ± SEM (B-D). **, p<0.01.

Figure S6.

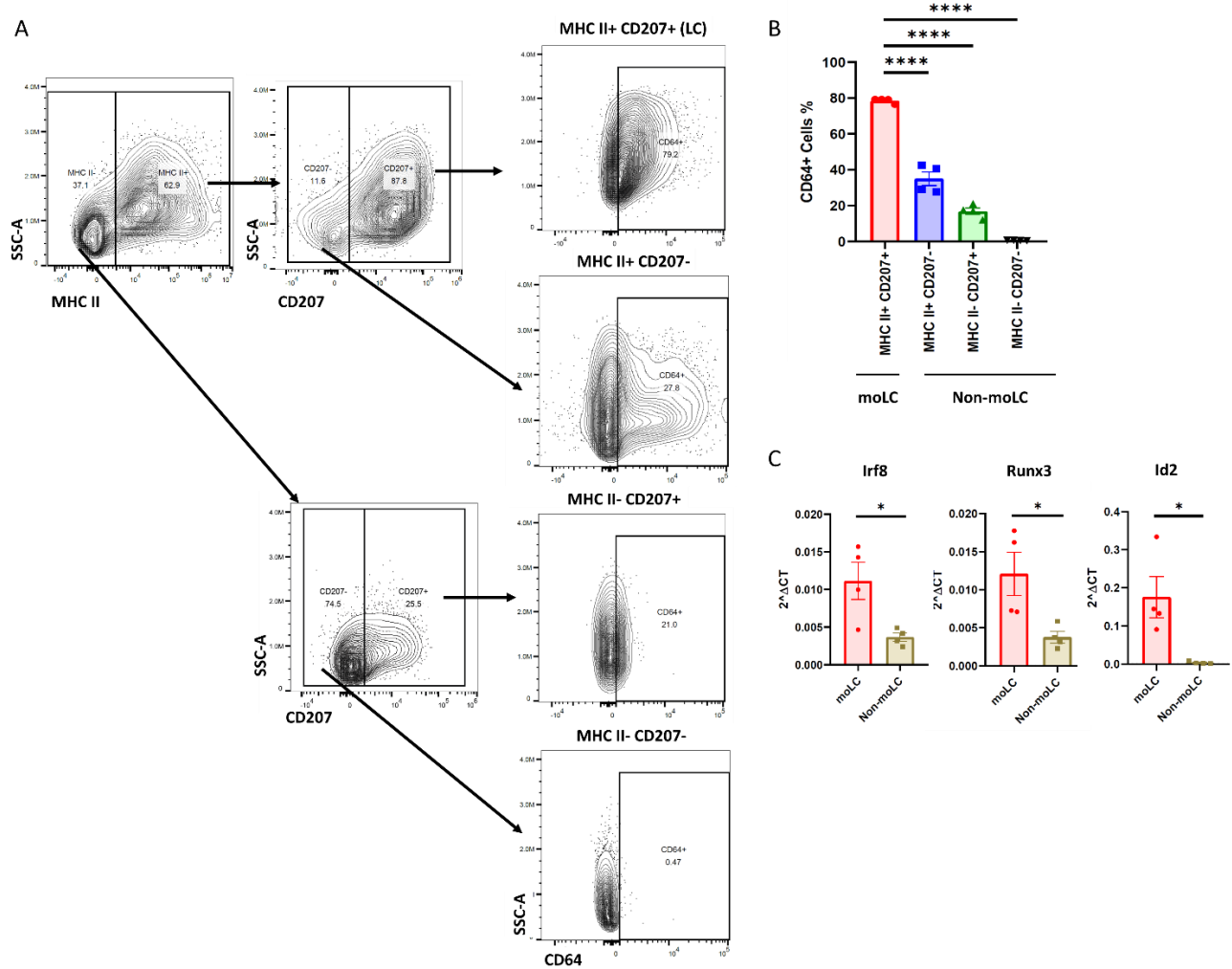


Figure S6. Characterization of monocyte-derived Langerhans cells developed from bone marrow.

Related to Figure 4. A) Representative flow cytometry figure showing expression levels of CD64 (marker of monocyte-derived cells) in LC cluster (MHC II+ CD207+) and other clusters with cells developed from bone marrow as described in Figure 3E. B) Quantification of CD64+ cells percentage in moLC cluster and other various clusters. C) qPCR of lineage-defining transcription factors of monocyte-derived cells (Irf8) and LCs (Runx3 and Id2) in moLCs and non-moLCs. p values determined by one-way ANOVA (B) followed by Tukey's post-hoc test and unpaired Student's T-test followed by Tukey's post-hoc test. Mean \pm SEM (B and C). *, p<0.05; ****, p<0.0001.

Figure S7.

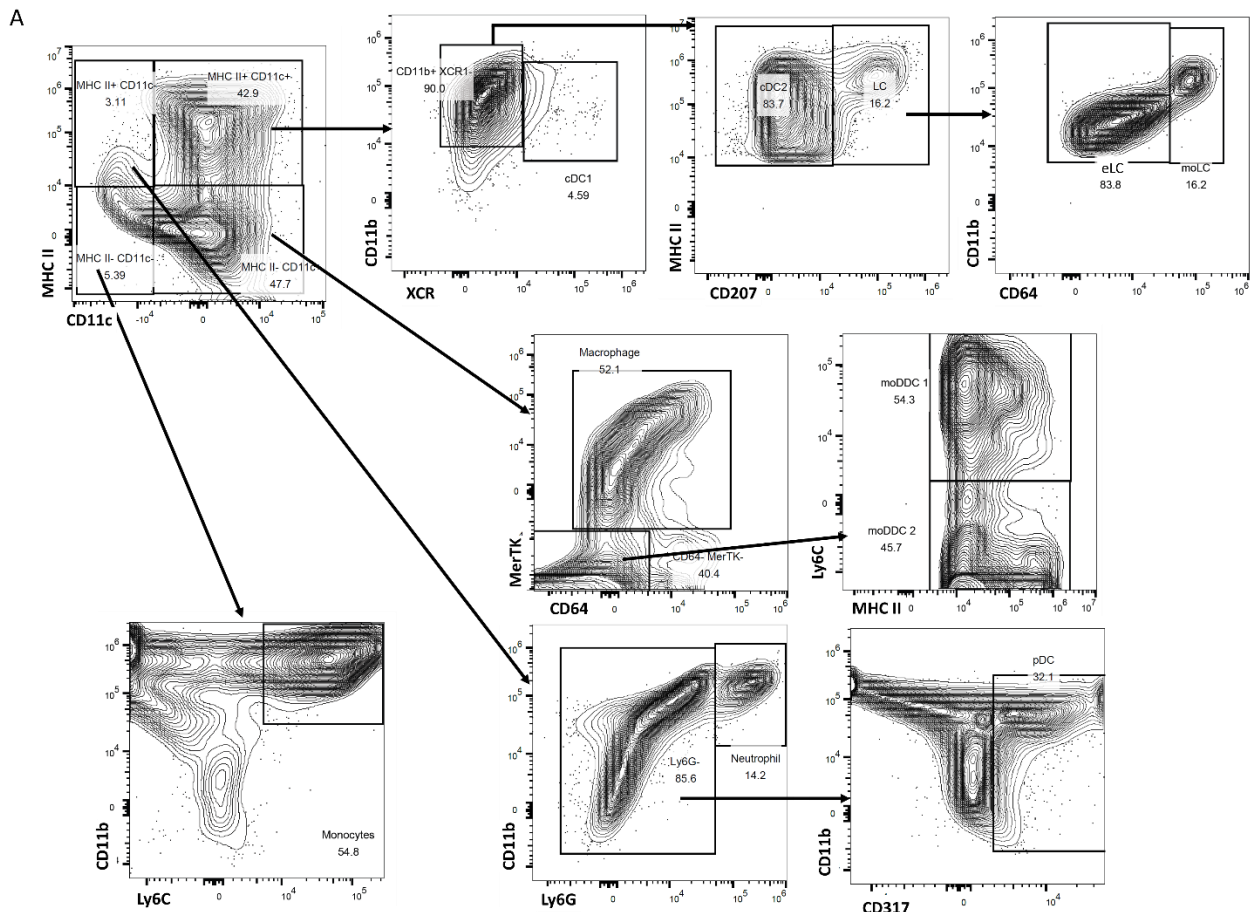


Figure S7. Gating strategy for identifying various cell clusters after spectral flow cytometry.

Related to Figure 5. A) Figures showing the gating strategy of identifying 10 different cell clusters (conventional dendritic cells 1, conventional dendritic cells 2, embryo Langerhans cells, monocyte-derived Langerhans cells, plasmacytoid dendritic cells, macrophages, monocyte-derived dendritic cells 1, monocyte-derived dendritic cells 2, neutrophils, and monocytes) after performing spectral flow cytometry.

Figure S8.

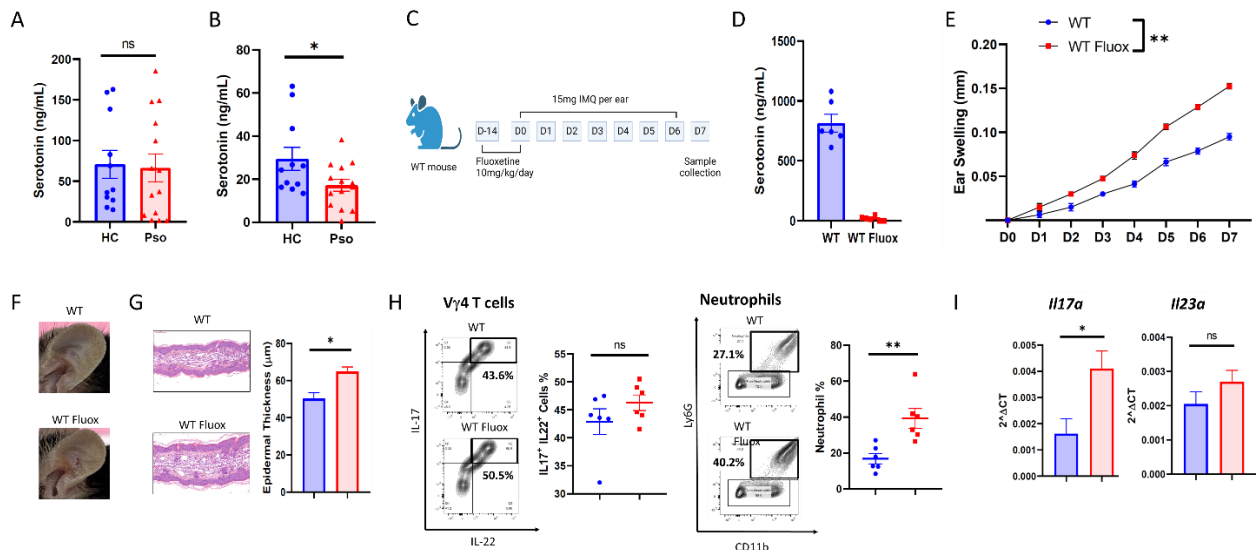


Figure S8. Platelet serotonin is lower in psoriatic patients and its deficiency is associated with exacerbated inflammation. A) Plasma serotonin of healthy controls (HC) (n=11) and psoriatic patients (Pso) (n=14). B) Serotonin of 1×10^6 platelets of HC (n=11) and Pso (n=14). C) Schematic showing the experimental plan to deplete platelet serotonin by chronic fluoxetine pre-treatment of mice. D) Serotonin levels of 2×10^6 platelets on Day 0 in wild type mice and wild type mice pre-treated with fluoxetine (n=6). E) Line chart showing changes in ear swelling of mice in their respective groups. F) Picture of mice ears on Day 7 in mice pre-treated with fluoxetine and their respective controls. G) H&E-stained slides of mice ears collected on Day 7 with quantification of epidermal thickness of the respective groups. H) Flow cytometry of IL17+ IL22+ $\text{V}\gamma 4$ T cells and neutrophils of mice ears collected on Day 7 of the respective groups. I) mRNA levels of pro-inflammatory cytokines of mice ears of the respective groups collected on Day 7. p values determined by two-way ANOVA (E) followed by Tukey's post-hoc test and unpaired Student's T-test. Mean \pm SEM (A-B and D-I). *, p<0.05; **, p<0.01; ns, non-significant.